JHEP|Reports

Transcriptional and functional HBV-specific CD8 T cell changes from disease to functional cure in HBeAg-negative chronic hepatitis B

Authors

Marzia Rossi, Andrea Vecchi, Camilla Tiezzi, …, Carlo Ferrari, Massimo Levrero, Carolina Boni

Correspondence

carolina.boni@unipr.it (C. Boni).

Graphical abstract

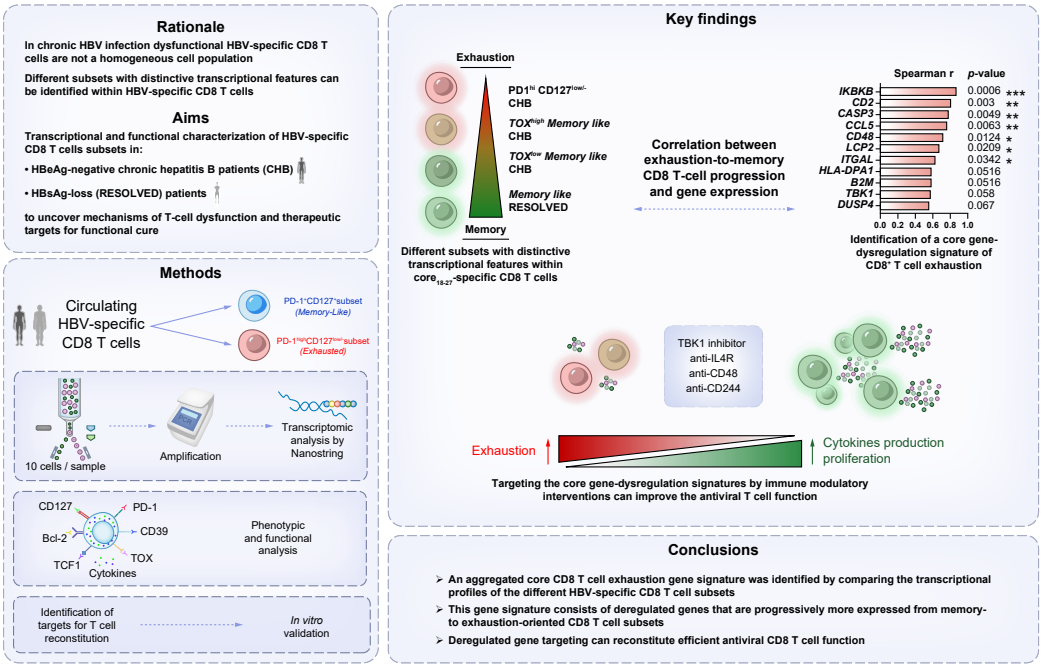

Highlights:

- In chronic HBV infection, dysfunctional HBV-specific CD8 T cells are not a homogeneous cell population.
- Different subsets with distinctive transcriptional features can be identified within HBV-specific CD8 T cells.
- A core CD8 T-cell exhaustion gene signature was identified by comparing transcriptional profiles of HBV-specific CD8 T-cell subsets.
- This signature includes genes progressively upregulated from memory-to exhaustion-oriented CD8 T-cell subsets.
- Deregulated gene targeting can reconstitute efficient antiviral CD8 T-cell function.

Impact and implications:

Exhausted HBV-specific CD8 T cells in chronic HBV infection are not a homogeneous population but comprise distinct subsets with differing capacities to control infection. This study identifies: (i) a transcriptional continuum of HBV-specific CD8 T-cell subsets spanning exhaustion to memory differentiation, reflecting disease progression and recovery in HBeAg-negative CHB; (ii) a core CD8 T-cell exhaustion gene signature characterized by progressively increased expression from memory-oriented to exhaustion-oriented subsets during active and resolution phases of disease; and (iii) the ability of targeted modulation of deregulated genes to restore antiviral CD8 T-cell function, with implications for the development of novel immune-based anti-HBV therapies. Overall, these findings advance our understanding of CD8 T-cell heterogeneity in chronic HBV infection and identify molecular targets for immunomodulatory strategies aimed at restoring CD8 T-cell functionality and achieving functional cure.

https://doi.org/10.1016/j.jhepr.2025.101705

Research article

JHEP|Reports

Transcriptional and functional HBV-specific CD8 T cell changes from disease to functional cure in HBeAg-negative chronic hepatitis B

Marzia Rossi[1,†], **Andrea Vecchi**[2,†], **Camilla Tiezzi**[1,†], Francesca Guerrieri[3,4,@], Marie Laure Plissonnier[3,4], Elisabetta Degasperi[5], Dana Sambarino[5], Diletta Laccabue[1], Arianna Alfieri[2], Elena Adelina Gabor[1], Amalia Penna[2], Valentina Reverberi[1], Anna Montali[1], Alessio Pelagatti[1], Sara Doselli[1], Benedetta Farina[1], Giuseppe Pedrazzi[6], Paola Fisicaro[2], Gabriele Missale[1,2], Pietro Lampertico[5,7], Carlo Ferrari[1,2], Massimo Levrero[3,4,8,9,10], Carolina Boni[1,2,*]

JHEP Reports **2026**. vol. 8 | 1–14

Background & Aims: In chronic HBV infection, HBV-specific CD8 T cells are dysfunctional and comprise distinct subsets defined by phenotype and antigen specificity. We aimed to characterize the transcriptional and functional features of HBV-specific CD8 T-cell subsets in patients with HBeAg-negative chronic HBV infection who were either viremic (CHB) or had achieved spontaneous or nucleos(t)ide analogue (NUC)–induced HBsAg loss (RES), to better elucidate HBV-specific CD8 T-cell dysfunction and identify potential molecular targets for functional cure.

Methods: Gene expression profiles of PD1^{hi}CD127$^{low/-}$ and PD1+CD127+ memory-like (*ML*) core$_{18\text{-}27}$-specific CD8 T-cell subsets were analyzed by Nanostring, adapted for low-input samples in 5 patients with HBeAg-negative CHB and 6 with RES. An expanded cohort of 23 patients with CHB and 22 with RES was evaluated for phenotypic and functional profiling. Selected deregulated genes were functionally validated in an additional cohort of 14 patients with HLA-A2-negative CHB.

Results: Analysis of 84 genes concurrently expressed across all CD8 T-cell subsets identified an 11-gene signature describing a progressive transition from exhaustion-oriented PD1^{hi}CD127$^{low/-}$ CD8 T cells in patients with CHB to memory-oriented *ML* CD8 cells in patients with RES, representing the two extremes of differentiation. Intermediate stages of memory differentiation were identified among *ML* CD8 T cells from patients with CHB, with high or low TOX expression (p <0.05 by Spearman's rank correlation). Higher frequencies of TOX^{low} *ML* CD8 cells in patients with CHB were associated with a greater serum HBsAg decline during NUC treatment compared to TOX^{high} *ML*CHB (Δ slope p value = 0.003). Targeting selected deregulated genes with specific immune modulators significantly enhanced cytokine production by CD8 T cells, with response rates ranging from 30% to 86% of patients.

Conclusions: Distinct exhaustion signatures characterize HBV-specific CD8 T-cell subsets and vary across disease phases. These findings support the development of individualized transcriptional and functional correction strategies and identify novel immune modulators with potential for immune-based anti-HBV therapies.

Introduction

In chronic HBV infection, HBV-specific CD8 T cells are dysfunctional due to the combined effect of different molecular mechanisms; this altered functionality has generally been referred to as T-cell exhaustion. Studies in the mouse model of LCMV (lymphocytic choriomeningitis virus) infection and in chronically HCV-infected patients have shown, however, that dysfunctional virus-specific CD8 T cells are highly heterogeneous, with distinct T-cell subsets exhibiting different levels of antiviral activity.[1–3] Similar functional heterogeneity has been observed in chronic HBV infection, where HBV-specific T-cell function appears to be shaped by different factors, including not only the phase of infection[4] and viral and antigen load, but also antigen specificity,[4–6] intrahepatic antigen distribution and modes of antigen recognition,[7,8] and the duration of infection.[9]

T-cell exhaustion is generally associated with induction of the transcription factor TOX following prolonged TCR stimulation by high antigen levels and is characterized by expression of multiple co-inhibitory receptors, altered transcriptional programs, and impaired effector function.[1] We recently described a CD8 T-cell exhaustion index based on multiparametric phenotypic staining (PD-1, CD127, TOX, CD39, Bcl-2, TCF-1),

* Corresponding author. Address: Department of Medicine and Surgery, University of Parma, Laboratory of Viral Immunopathology, Unit of Infectious Diseases and Hepatology, Azienda Ospedaliero-Universitaria di Parma, Via Gramsci 14, 43126 Parma, Italy.
E-mail address: carolina.boni@unipr.it (C. Boni).
† These authors contributed equally to this work.
@ Present address: UMR-S 1193 INSERM/Université Paris-Saclay; Centre Hépato-biliaire Hôpital Paul Brousse, Villejuif, France
https://doi.org/10.1016/j.jhepr.2025.101705

which enables quantification of overall CD8 T-cell dysfunction in individual treatment-naïve HBeAg-negative CHB patients and predicts the likelihood of *in vitro* functional restoration.[10] This phenotypic profiling also identified distinct circulating HBV-specific CD8 T-cell subsets: one detectable in a limited proportion of viremic patients (PD1^{hi}CD127$^{low/-}$) and another (PD1+CD127+) present in both actively infected and cured patients.

By inference with other chronic infections,[2,3] the PD1^{hi}CD127$^{low/-}$ CD8 T-cell subset is thought to represent the most terminally exhausted population; however, comprehensive transcriptional and functional characterization of these cells in chronic viremic HBeAg-negative hepatitis B is still lacking. Conversely, the PD1+CD127+ subset has been defined as a "memory-like" T-cell subset, yet its presence in both chronic viremic patients and in patients able to control virus replication suggests a possible transcriptional and functional plasticity of these cells which is worth investigating.

The novelty of our study lies in its focus on highly viremic patients with active disease and severely exhausted CD8 T cells – cells that are particularly challenging to isolate – as well as on patients who achieved functional cure following spontaneous or nucleos(t)ide analogue (NUC)–induced HBsAg loss.

We focused on core$_{18-27}$-specific T cells to enable comparisons across disease stages, given the exceedingly low frequencies of polymerase- and envelope-specific CD8 T cells in patients with CHB.

Here, we combined low-input Nanostring-based gene expression profiling of individual HBV-specific CD8 T-cell subsets (1–10 cells per sample) with functional/phenotypical characterization, T cell protein and functional validation by flow cytometry to gain mechanistic insight and identify strategies to selectively target CD8 T-cell subsets with different degrees of exhaustion.

Patients and methods

Study participants

A total of 45 HLA-A2+ patients (Table 1), with detectable frequencies of core$_{18-27}$-specific CD8 T cells, were enrolled, comprising: 23 patients with HBeAg-negative CHB, eligible for antiviral treatment according to EASL CPGs;[11] 22 patients with CHB who achieved persistent HBsAg loss either spontaneously or by NUC therapy (resolved, RES).

An additional 14 HLA-A2–negative treatment-naïve CHB patients and 5 resolved patients were enrolled to perform further *in vitro* functional validation of the deregulated genes (Table 2). Eight healthy individuals were enrolled as controls.

Cell sorting

After peripheral blood mononuclear cell thawing, CD8 T cells were isolated and labeled with 7-AAD, anti-CD3, anti-CD8, anti-CD279 (PD1), anti-CD127 antibodies, and the core$_{18-27}$-HLA class I complex dextramer.

Dextramer-positive CD8 T cells were sorted with a FACSAria III Cell Sorter, and ten cells/sample were collected directly in single-cell lysis solution for Nanostring experiments per each condition: 10 PD1^{hi}CD127$^{low/-}$ HBV-specific CD8 T-cell subset, 10 PD1+CD127+ HBV-specific CD8 T-cell subset, 10 total HBV-specific CD8 T cells. We decided to perform transcriptional analysis with 10 cells per subset since they can likely be isolated in all samples and represent the cell number validated in our previous studies[12] as a reliable threshold for reproducible Nanostring experiments.

Nanostring analysis

The expression of 579 immunology-related human genes and an additional panel of 30 genes[12] was evaluated in 10 sorted T cells per each condition according to the "nCounter XT Gene Expression assay for single cells" Nanostring protocol with minor modifications.[12]

Identification of differentially expressed genes using effect size calculation

To establish relevant differentially expressed genes between groups, we relied on the estimation of the effect size.[13] For our data, we chose the "large effect" threshold as the discriminant for the list of genes of interest to be used for a more stringent evaluation.

Assessment of gene variability by the IQR on *ML* subsets

To analyze the degree of gene variability of memory-like (*ML*) subsets derived from treatment-naïve CHB or RES patients, data dispersion was quantified using the IQR.

Phenotypic analysis of HBV-specific CD8 T cells

Dextramer-positive CD8 T cells were stained with antibodies to cytokine receptors (CD127), anti-apoptosis/cell survival (Bcl-2 and TCF-1) and T-cell exhaustion (PD-1, TOX and CD39) markers.

Protein expression levels of the identified deregulated genes were tested with antibodies to IL4R and CD244 by flow cytometry.

Ex vivo functional assessment of HBV-specific CD8 T cells

Intracellular cytokine staining for IFN-γ and TNF-α was performed on dextramer+CD8+ T cells following stimulation with PMA (100 ng/ml) and ionomycin (1 μg/ml) for 4 h.

In vitro T-cell expansion and treatment with immunomodulators

T-cell cytokines (IFN-γ, TNF-α and IL-2) were tested by intracellular cytokine staining, as previously described[10] on short-term T-cell lines treated with the following compounds: a TBK1 inhibitor; anti-CD48 and anti-CD244 antibodies; and an anti-IL4R antibody.

Additional materials and methods

A full description of all methods and statistical analysis is provided in the supplementary materials section.

Results

Transcriptional profiling of HBV-specific CD8 T cells from CHB and RES patients

The comparison of global transcriptional profiles of total dextramer-stained core$_{18-27}$-specific CD8 T cells sorted from

Table 1. Demographic and clinical details of different HLA-A2+ patient categories.

Patient ID	Sex	Age (years)	Genotype	Experiments*	Therapy	HBsAg (IU/ml)	Anti-HBs (IU/ml)	ALT (IU/L)	HBV DNA (IU/ml)
CHB									
CHB 1	M	35	D	Nanostring/cytokines/phenotype	Naïve	1,932	-	136	237,528
CHB 2	F	40	D	Nanostring/cytokines/phenotype	Naïve	608	-	93	881,000
CHB 3	M	34	D	Nanostring/cytokines/phenotype	Naïve	4,085	-	85	3,497,520
CHB 4	F	40	D	Nanostring/cytokines/phenotype/validation	Naïve	5,398	-	168	842,528
CHB 5	F	42	C	Nanostring/cytokines/phenotype/validation	Naïve	144	-	51	6,800,000
CHB 6	M	36	B	Cytokines	Naïve	3,472	-	607	8,132,680
CHB 7	F	51	D	Cytokines/phenotype/validation	Naïve	482	-	43	66,400
CHB 8	F	57	A	Cytokines/phenotype	Naïve	4,600	-	65	229,402
CHB 9	M	54	D	Cytokines/phenotype	Naïve	694	-	183	9,856
CHB 10	F	43	D	Cytokines/phenotype	Naïve	714	-	30	11,453
CHB 11	M	44	D	Cytokines/phenotype	Naïve	8,819	-	49	20,700
CHB 12	M	64	A	Cytokines/phenotype	Naïve	185	-	33	5,140
CHB 13	F	29	D	Cytokines/phenotype	Naïve	5,140	-	21	31,721
CHB 14	F	57	D	Cytokines/phenotype	Naïve	19,679	-	34	509,000
CHB 15	M	34	D	Cytokines/phenotype/validation	Naïve	2,752	-	40	86,620
CHB 16	M	54	D	Cytokines/phenotype	Naïve	4,775	-	68	153,246
CHB 17	M	52	D	Cytokines/phenotype/validation	Naïve	2,662	-	40	21,331
CHB 18	M	44	D	Cytokines/phenotype	Naïve	3,736	-	146	1,400,591
CHB 19**	F	66	D	Cytokines/phenotype	Naïve	98	148	23	7,744
CHB 20	F	26	A	Cytokines/phenotype	Naïve	7,171	-	12	3,380
CHB 21	M	38	D	Phenotype/validation	Naïve	5,031	-	57	110,009
CHB 22	M	50	D	Validation	Naïve	2,940	-	35	9,733
CHB 23	M	71	D	Validation	Naïve	3,097	-	23	5,030
Resolved									
RES 1	M	79	D	Nanostring/cytokines/phenotype	NUC	-	4	19	-
RES 2	M	65	D	Nanostring/phenotype	NUC	-	2	19	-
RES 3	M	43	A	Nanostring/cytokines/phenotype/validation	NUC	-	506	17	-
RES 4	M	38	D	Nanostring/cytokines/phenotype	NUC	-	190	19	-
RES 5	M	64	N/A	Nanostring	-	-	55	38	-
RES 6	F	69	N/A	Nanostring/cytokines/phenotype	-	-	66	26	-
RES 7	M	81	N/A	Cytokines	NUC	-	33	14	-
RES 8	M	57	D	Cytokines	NUC	-	26	28	-
RES 9	F	46	F	Cytokines/validation	NUC	-	173	20	-
RES 10	M	64	A	Cytokines/validation	NUC	-	325	23	-
RES 11	M	48	N/A	Phenotype	NUC	-	>1,000	29	-
RES 12	M	59	N/A	Cytokines/validation	-	-	45	30	-
RES 13	M	49	N/A	Cytokines	-	-	+	36	-
RES 14	M	60	N/A	Cytokines	-	-	270	31	-
RES 15	F	73	N/A	Cytokines/phenotype	-	-	7	15	-
RES 16	F	41	N/A	Cytokines/phenotype	-	-	451	11	-
RES 17	M	58	N/A	Phenotype/validation	-	-	47	48	-
RES 18	F	59	D	Phenotype	-	-	20.11	16	-
RES 19	F	67	N/A	Phenotype	-	-	11.2	19	-
RES 20	M	65	N/A	Validation	NUC	-	n.d.	32	-
RES 21	M	60	N/A	Validation	NUC	-	2	31	-
RES 22	M	36	N/A	Validation	NUC	-	216.91	23	-

ALT, alanine aminotransferase; CHB, chronic hepatitis B; NA, not available; NUC, nucleos(t)ide analogues; RES, resolved HBV infection.

*Assay performed in the indicated patients.

**Patient followed for >10 years; CHB diagnosed by liver biopsy; fluctuations of ALT (from normal to slightly elevated) and viremia (from 5,000 IU/ml to 40,000 IU/ml) levels; recent detection of anti-HBs combined with HBsAg.

Table 2. Demographic and clinical details of different HLA-A2- patient categories.

Patient ID	Sex	Age (years)	Genotype	Experiments*	Therapy	HBsAg (IU/ml)	Anti-HBs (IU/ml)	HBeAg	ALT (IU/L)	HBV DNA (IU/ml)
CHB										
CHB 24	M	50	D	T cell functional validation	Naïve	11,557	-	-	24	12,102
CHB 25	M	77	A	T cell functional validation	Naïve	91,270	-	+	60	442,709,600
CHB 26	M	48	D	T cell functional validation	Naïve	17,589	-	-	50	3,880,200
CHB 27	M	20	N/A	T cell functional validation	Naïve	3,761	-	-	24	246
CHB 28	M	37	D	T cell functional validation	Naïve	65,626	-	-	26	169,601
CHB 29	M	23	D	T cell functional validation	Naïve	9,329	-	-	26	5,837
CHB 30	M	36	D	T cell functional validation	Naïve	7,458	-	-	25	47,946
CHB 31	M	47	D	T cell functional validation	Naïve	8,181	-	-	212	150,300
CHB 32	M	64	D	T cell functional validation	Naïve	228	-	-	19	116,997
CHB 33	M	59	D	T cell functional validation	Naïve	55,988	-	+	72	349,480,200
CHB 34	F	42	D	T cell functional validation	Naïve	12,539	-	-	90	31,836,000
CHB 35	M	81	N/A	T cell functional validation	Naïve	11,695	-	-	116	2,866,690
CHB 36	M	37	D	T cell functional validation	Naïve	182	-	-	27	11,995
CHB 37	F	29	D	T cell functional validation	Naïve	30,606	-	+	59	135,171,000
Resolved										
RES 23	M	44	N/A	T cell functional validation	NUC	-	97	-	30	-
RES 24	M	79	N/A	T cell functional validation	NUC	-	2	-	10	-
RES 25	F	75	D	T cell functional validation	NUC	-	46	-	44	-
RES 26	M	41	N/A	T cell functional validation	NUC	-	45	-	38	-
RES 27	F	63	N/A	T cell functional validation	NUC	-	97	-	20	-

ALT, alanine aminotransferase; CHB, chronic hepatitis B; NA, not available; NUC, nucleos(t)ide analogues; RES, resolved HBV infection.
*Assay performed in the indicated patients.

the peripheral blood of patients in the chronic (n = 5) and resolution (n = 6) phases of chronic HBV infection (Fig. 1A) revealed a clear segregation of the two patient groups by unsupervised analysis of the 263 expressed genes (Fig. 1B). Some heterogeneity within each group was expected, reflecting differences in the time elapsed between antigen loss and study enrollment among RES individuals, as well as the variable degrees of infection and disease severity typically observed in patients with CHB. Despite these potential limitations, 65 differentially expressed genes (DEGs) between patients with chronic and resolved infections were identified (Fig. 1C) and principal component analysis of these 65 genes confirmed the evident segregation of CHB and RES (Fig. 1D).

Several of the most upregulated genes in patients with CHB have been reported to be deregulated in animal and human models of T-cell dysfunction.[1–4,12,14–17] These included genes involved in inflammatory processes (*MAP4K2, CCL5, IL16, MYD88, GBP1, GBP5*) and T-cell activation (*TFRC, LCK, CD81, CD2, DDB1*), transcription factor-encoding genes (*IRF1, STAT1, ILF3*), the NF-κB signaling-mediator MALT1, exhaustion-related genes involved in inhibitory pathways (*SELPLG, CD244, CTLA4, ENTPD1, LAG3, LILRA5, CD48*), autophagy and apoptosis (*ATGI6L1, BAX, FADD, RARRES3*) (Fig. 1E). Additional dysregulated genes were related to intracellular signaling and cell cycle control (*LRPPRC, PRKCD, MAPKI4, IKZF2, LEF1*), effector functions (*GZMA, GZMB*), and mitochondrial (*FIS1, NDUFA6, NDUFA4, TIMM23, PHB2, UQCRC1*) and proteasome (*PSME1, PSMB10, PSMD3*) pathways (Fig. 1C).

In contrast, fewer genes were upregulated in RES patients and downregulated in patients with CHB; these genes were mainly associated with immune regulation (*SOCS1, CD5, IL6ST*) and T-lymphocyte migration (*CXCR3*)[18–21] (Fig. 1E).

Overall, transcriptional profiling of total HBV-specific CD8 T cells revealed predominant upregulation during the chronic phase of genes involved in inflammation, activation, and inhibitory pathways, whereas genes promoting immune regulation and responsiveness were preferentially upregulated during the resolution phase of chronic HBV infection.

Differential transcriptional profiles of *ML* PD1+CD127+ HBV-specific CD8 T cells in CHB (*ML*-CHB) and resolved patients (*ML*-RES)

As already described,[10] conventional memory HBV-specific T cells (PD-1-/CD127+) generated after spontaneous resolution of acute HBV infection were not present in patients who achieved functional cure following chronic HBV carriage. Thus, we focused our analysis on *ML* PD1+CD127+ HBV-specific CD8 T cells to elucidate whether their transcriptional profile might differ depending upon the phase of infection. Using the Kruskal-Wallis test, we identified 17 genes with significantly different expression levels in *ML* CD8 T cells derived from 4 CHB and 6 RES patients (Fig. 2A-C).

In addition, a significantly greater degree of heterogeneity was observed in CHB *vs*. RES patients by applying an IQR calculation after z-score normalization (Fig. 2D; p <0.0001 and medium effect size r = 0.36), in line with the assumption that successful control of HBV infection should result in a more homogeneous population of *ML* cells.[10]

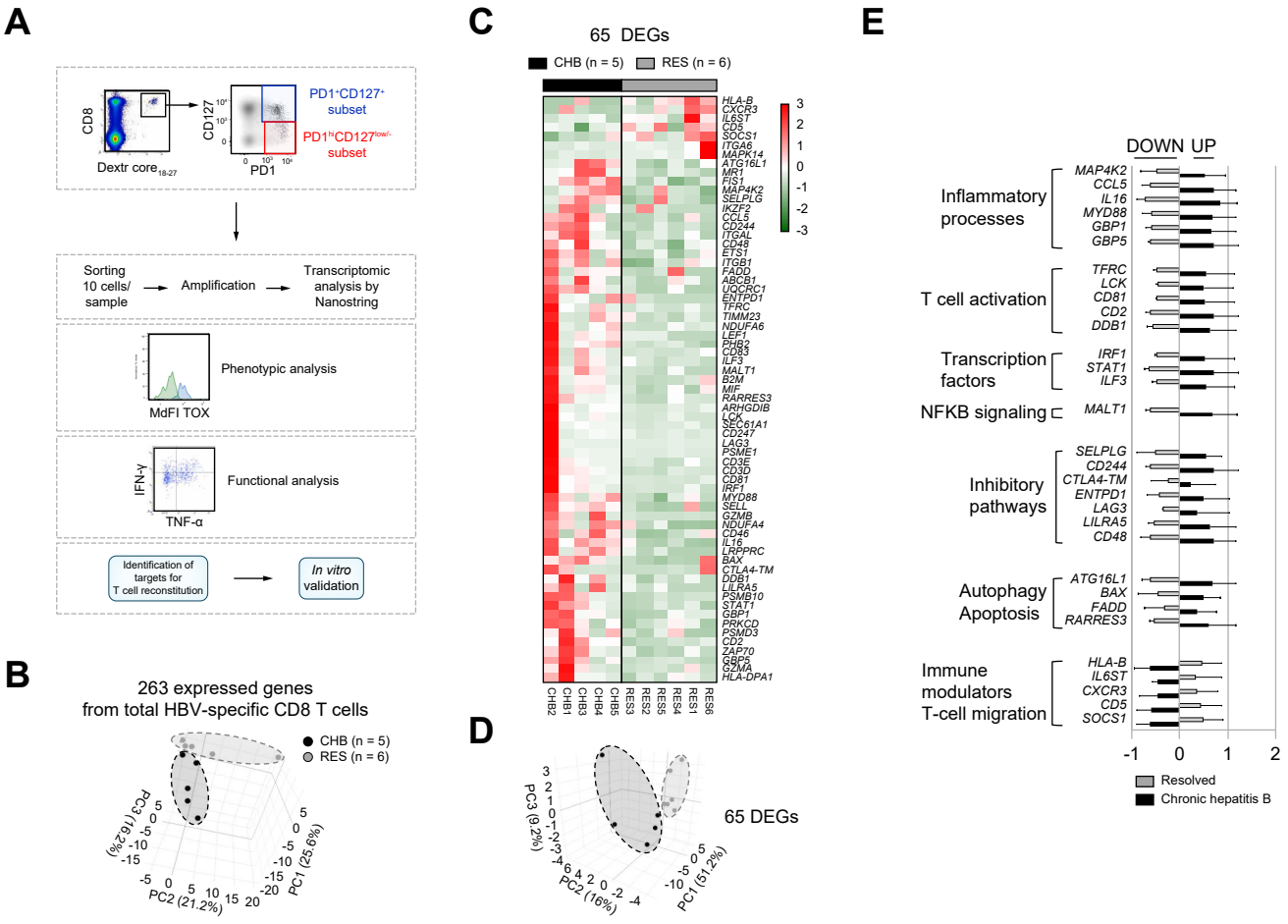

Fig. 1. Gene-expression profiling of total core$_{18-27}$-specific CD8+ T cells from CHB and RES patients. (A) Overview of the experimental design. (B) Patient group correlation by unsupervised PCA of all 263 expressed genes identified in total HBV-specific CD8 T cells from patients with chronic (n = 5) and resolved (n = 6) HBV infections. (C-D) Hierarchical-clustering (C) and PCA representation (D) of the 65 DEGs identified by the Kruskal-Wallis test. Data were centered and normalized before clustering (z-score); upregulated and downregulated genes are shown in red and green, respectively. (E) Bar-plot representation of some selected DEGs (mean expression value plus SEM for each patient category) grouped according to their respective functions; upregulated (black) and downregulated (grey) genes are shown for each patient. CHB, chronic hepatitis B; DEG, differentially expressed gene; PCA, principal component analysis; RES, resolved HBV infection.

Next, we asked whether some of the 65 genes differentially expressed in total HBV-specific CD8 T cells from CHB *vs*. RES patients (Fig. 1C) overlapped with the 17 DEGs distinguishing the *ML* T-cell subsets of chronic and resolved patients. Of note, 6 common DEGs (Fig. 2E) were identified with a concordant trend to upregulation in CHB *vs.* RES patients in both comparisons (Fig. 2F). These 6 genes are involved in inhibitory pathways (CD48), pro-inflammatory processes (CCL5), as well as T-cell activation (CD2, MR1, ZAP70, ABCB1), and their deregulation has previously been associated with dysfunction/exhaustion in other models of chronic infection and inflammation (Table S2). Additional genes upregulated in *ML*-CHB are related to NF-KB (IKBKB), TCR-activated tyrosine kinase (LCP2) and cytokine receptor (IL2RG) signaling, effector (GZMK) and differentiation processes (IL7R), as well as apoptosis (CRADD, CASP3, CUL9). The transcription factor *NFIL3*, involved in Treg cell function and stability, as well as the inhibitory molecules PDCD1 and LAIR1 were upregulated in the *ML*-RES subset (Fig. S1; Table S2). The finding of PDCD1 upregulation is rather unexpected, although the variable role that PD-1 can play in different settings – exhaustion *vs.* activation – can make the interpretation of transcriptional upregulation quite controversial, especially if not supported at the protein level, as in our study where protein expression was not significantly different between *ML*-CHB and *ML*-RES.

Taken together, these results indicate that *ML* HBV-specific CD8 T cells, although detectable in both chronic and resolved patients, differ at the transcriptional level in relation to activity or successful control of infection.

Exhaustion-related gene enrichment in the PD1^{hi}CD127$^{low/-}$ HBV-specific CD8 T-cell subset

The HBV-specific PD1^{hi}CD127$^{low/-}$ CD8 T-cell subset, which is only present in a proportion of treatment-naïve patients with CHB, is thought to be terminally differentiated towards dysfunction/exhaustion.[2,3,10] In patients CHB3 and CHB5, only *ML* PD1+CD127+ CD8 T cells were detected, whereas in patients CHB2 and CHB4 both PD1+CD127+ and PD1^{hi}CD127$^{low/-}$ subsets were present (Fig. 1A), enabling analysis of their transcriptional profile.

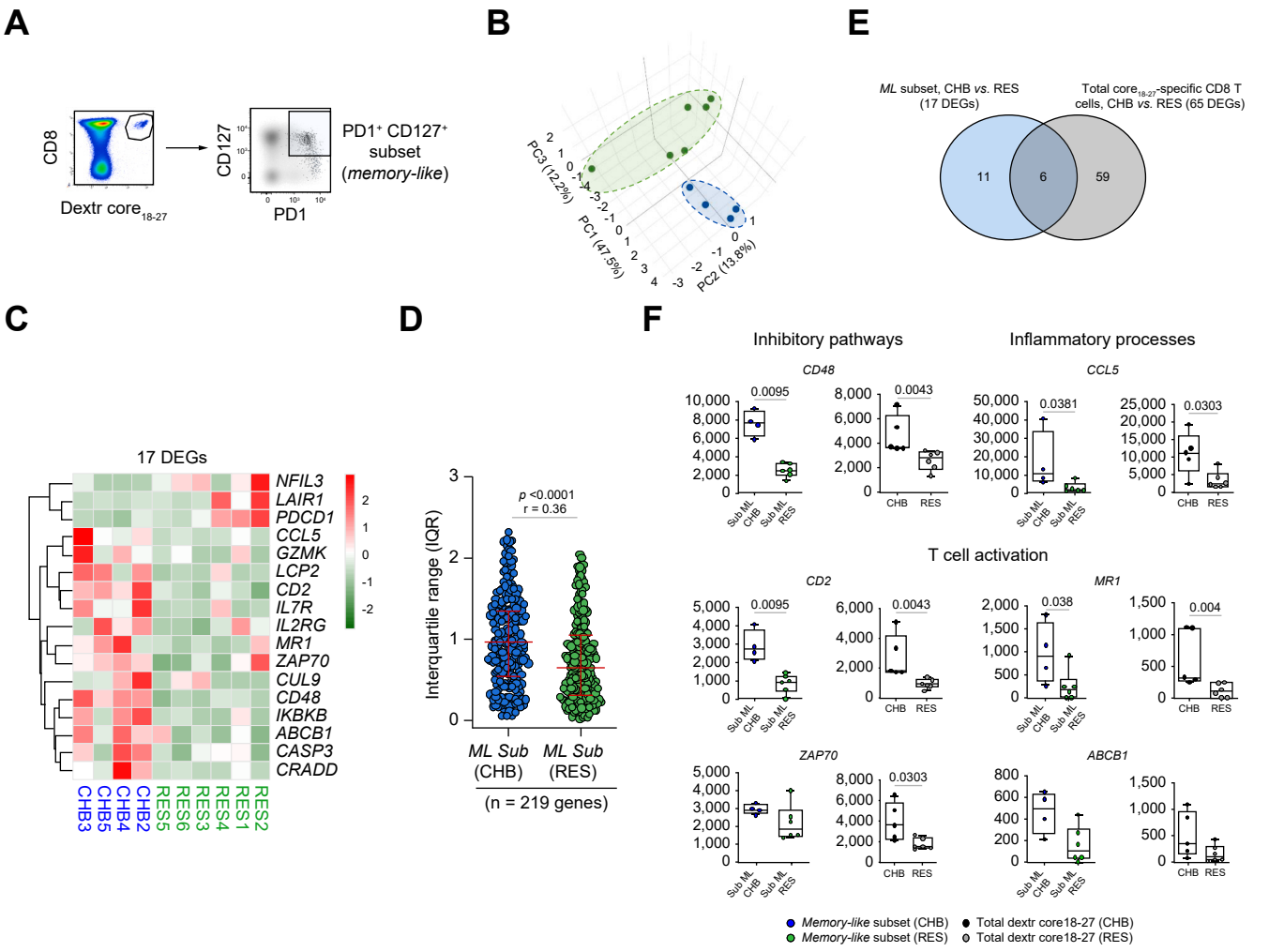

Fig. 2. Gene-expression profiling of *ML* HBV-specific CD8+ T-cell subsets from chronic and resolved patients. (A) Gating strategy to identify the *ML* PD1+CD127+ HBV-specific CD8 T-cell subset. (B) PCA and (C) Hierarchical-clustering representation of the 17 DEGs in PD1+CD127+ CD8 T cells from patients with chronic (n = 4, blue) and resolved (n = 6, green) HBV infections. Data were centered and normalized before clustering (z-score); upregulated and downregulated genes are shown in red and green, respectively. (D) Transcriptomic variability within *ML*-CHB (blue dots) and *ML*-RES (green dots) subsets, as shown by scatter plot representation displaying the IQR distribution of each gene. Median, 25th and 75th percentile values of IQR are shown. Statistics by Wilcoxon matched-pairs signed rank test (p <0.0001; medium effect-size r = 0.36). (E) Venn diagram of the DEGs derived from the comparison of *ML* subsets (light blue, n = 17) and total core$_{18-27}$-specific CD8 T cells (grey, n = 65) of chronic *vs*. resolved. The overlapping area represents genes shared between the two DEG lists (n = 6). (F) Overlapping DEGs (n = 6) are illustrated as box-and-whisker plots (with median and min-max values), according to their respective functions. Each dot represents an individual patient (blue and green dots indicate *ML*-CHB and *ML*-RES, respectively; black and grey indicate total dextr-core$_{18-27}$ T cells from CHB and RES patients, respectively); statistics by the Mann-Whitney *U* test. CHB, chronic hepatitis B; DEG, differentially expressed gene; ML, memory-like; PCA, principal component analysis; RES, resolved HBV infection.

We first compared the transcriptional profiles of the PD1^{hi}CD127$^{low/-}$ CD8 T cells from CHB2 and CHB4 patients with the *ML* PD1+CD127+ CD8 T cells derived from either the 6 RES (Fig. 3A, left panel) or the 4 CHB patients (Fig. 3A, right panel) and we identified 36 and 33 DEGs, respectively. Notably, we found only 15 genes in common (rectangular frame at the top of the heatmaps in Fig. 3A; upper radar plot and Venn diagram in Fig. 3B; panel A in Fig. S2), further confirming that *ML*-CHB and *ML*-RES largely differ in their transcriptional programs, as already suggested by the results of the direct comparison shown in Fig. 2. Focusing on the 21 non-overlapping DEGs in the comparison of *ML*-RES *vs.* PD1^{hi}CD127$^{low/-}$ T cells (Venn diagram, Fig. 3B; panel B in Fig. S2), both the heatmap and the radar plot shown in the left part of Fig. 3B underline their largely homogeneous downregulation in *ML*-RES T cells. Conversely, the 18 non-overlapping genes (Heatmap, Fig. 3A; Venn diagram, Fig. 3B) deriving from the comparison of PD1^{hi}CD127$^{low/-}$ *vs. ML*-CHB cells showed more heterogeneous expression levels with a more mixed representation of up- and downregulated genes among the two subsets (radar plot, right part of Fig. 3B; panel C in Fig. S2). These results suggest a greater transcriptional

distance between PD1^{hi}CD127$^{low/-}$ CD8 T cells and *ML* CD8 T cells from resolved compared with chronic patients, consistent with maximal dysfunction of PD1^{hi}CD127$^{low/-}$ CD8 cells and maximal transcriptional and functional recovery of *ML*-RES cells.

Assuming that the 65 DEGs in the comparison of total core$_{18-27}$-specific CD8 T cells from CHB and RES patients define the transcriptional distance between CD8 dysfunction on one extreme and recovered CD8 functionality on the other, the number of these DEGs in common with the 36 DEGs derived from the comparison of PD1^{hi}CD127$^{low/-}$ *vs. ML*-RES CD8 T cells should be greater than the number in common with the 33 DEGs derived from the comparison of PD1^{hi}CD127$^{low/-}$ *vs. ML*-CHB CD8 T cells. In line with this assumption, we found that 16 of the 36 DEGs (44%) from PD1^{hi}CD127$^{low/-}$ *vs. ML*-RES cells appeared to be in common and concordantly upregulated with the 65 DEGs (Fig. 3C, left box), as opposed to only 6 of the 33 DEGs (18.2%) derived from the PD1^{hi}CD127$^{low/-}$ *vs. ML*-CHB comparison (Fig. 3C, right box) (p = 0.0124 by McNemar's test). These shared DEGs include chemokines, genes involved in pro-inflammatory processes (*CD2, CCL5, MAP4K2, STAT1, ITGAL*), intracellular signaling (*PRKCD*), inhibitory checkpoint pathways (*CD48*) and cytotoxic effector functions (*GZMA* and *GZMB*) (Fig. 3C, left box; Table S2). These observations again indicate that PD1^{hi}CD127$^{low/-}$ CD8 T cells and *ML*-RES T cells represent the extremes of the spectrum from exhaustion to memory with *ML*-CHB in an intermediate position (Fig. 3C, right scheme). Of note, 20 additional DEGs were identified by comparing the most distant PD1^{hi}CD127$^{low/-}$ and *ML*-RES subsets (Fig. 3C, left part and Table S2). Some of these genes may be part of a more comprehensive CD8 exhaustion signature identified by combining DEGs derived from the comparison of total HBV-specific CD8 T cells from patients in the active and resolution phases of chronic HBV infection and of PD1^{hi}CD127$^{low/-}$ *vs. ML*-RES CD8 T cells.

In summary, the transcriptional analysis of the PD1^{hi}CD127$^{low/-}$ HBV-specific CD8 T-cell subset reveals an enrichment in exhaustion-related genes compared to the *ML* PD1+CD127+ subsets, which is more pronounced when the comparison is focused on *ML*-RES. In addition, the comparison between PD1^{hi}CD127$^{low/-}$ and *ML* CD8 T cells from chronic and resolved patients confirms that *ML* CD8 T cells can adopt distinct differentiation programs depending on the clinical context.

Phenotypic analysis enables further dissection of the *ML* PD1+CD127+ HBV-specific CD8 T-cell subset in patients with CHB

PD1+CD127+ and PD1^{hi}CD127$^{low/-}$ core$_{18-27}$-specific CD8 T cells from CHB and resolved patients were analyzed *ex vivo* by flow cytometry in a larger population of 21 patients with CHB and 18 resolved patients to assess cytokine production and the expression of TOX and TCF1 transcription factors, Bcl-2 and the checkpoint molecule CD39. Patients previously analyzed for their transcriptional profile were included in this expanded cohort.

TOX expression was significantly higher in PD1^{hi}CD127$^{low/-}$ than in *ML*-CHB and *ML*-RES (Fig. 4A). Notably, the quantification of TOX protein levels allowed us to distinguish, using a median fluorescence intensity threshold value of 640, corresponding to the maximum value observed in the resolved patient cohort (red dotted line in Fig. 4A), two different populations within the *ML* PD1+CD127+ subset of patients with CHB (*ML*-TOX^{low} CHB and *ML*-TOX^{high} CHB). Conversely, Bcl-2 expression was significantly reduced in PD1^{hi}CD127$^{low/-}$ T cells in comparison with the *ML*-TOX^{high} CHB and *ML*-RES CD8 cells. Differences between distinct T-cell subsets were less evident for CD39 and TCF-1 (Fig. S3).

In line with the phenotypic profiling, PD1^{hi}CD127$^{low/-}$ cells from chronic patients produced lower levels of cytokines compared to *ML*-TOX^{low} CHB and *ML*-RES cells. Moreover, cytokine production was higher in *ML*-TOX^{low} and *ML*-RES T cells compared to *ML*-TOX^{high} cells (Fig. 4B). A statistically significant negative correlation between cytokine production and TOX levels was also observed (Fig. 4C).

As shown in Fig. 4D, unsupervised analysis grouped CHB3 and CHB5, which exhibit low TOX levels, together, whereas CHB2 and CHB4, with higher TOX expression, clustered separately. Thus, the transcriptional profile of *ML* cells from chronic patients with low TOX levels appeared to be distinct from that of *ML* cells from chronic patients with higher TOX expression.

Of note, PD1^{hi}CD127$^{low/-}$ T cells were present in CHB2 and CHB4 patients along with TOX^{high} *ML* CD8 T cells, whereas PD1^{hi}CD127$^{low/-}$ T cells were not detected in CHB3 and CHB5 patients with TOX^{low} *ML* cells. Forty-three DEGs were found in the comparison between TOX^{low} and TOX^{high} *ML* CD8 T cells, showing clear segregation according to TOX levels (Fig. 4D), and aligning along the proposed trajectory, as illustrated by unsupervised principal component analysis (Fig. 4E). TOX^{high} *ML* CD8 T cells showed a significant upregulation of genes associated with apoptosis, NF-kB signaling and inhibitory pathways, suggesting a more dysfunctional immune profile, compared to *ML*-TOX^{low} CD8 T cells (Fig. 4F; Table S2). Additional genes upregulated in *ML*-TOX^{high} CD8 T cells are involved in cell cycle modulation (*CDKN1B, DUSP4*) and regulatory pathways known to promote T-cell exhaustion and immunosuppression (*TGFB1, XBP-1, IL4R, IL21R, CD44, CD59*). Finally, the upregulation of SLC2A1/Glut1 in *ML*-TOX^{high} CD8 T cells may reflect a critical glucose metabolic adaptation of more dysfunctional *ML*-TOX^{high} T cells (Fig. 4F; Table S2).

Interestingly, a statistically significant inverse correlation between TOX expression and frequencies of individual *ML*-CHB subsets was also observed (Fig. 4G). To understand whether the presence of *ML*-TOX^{low} cells in individual patients with CHB predicts a higher likelihood of HBsAg decline during NUC treatment, we conducted a longitudinal follow-up of serum HBsAg levels. CHB patients with *ML*-TOX^{low} CD8 T cells displayed a significantly better serum HBsAg decline upon NUC treatment over time compared to those with *ML*-TOX^{high} cells, suggesting that patients with *ML*-TOX^{low} CD8 T cells may have an increased probability of resolving CHB (Fig. 4H; Δ slope p value = 0.003 by linear mixed-effects model analysis; details in the supplementary materials).

Thus, TOX levels enable the identification of distinct subpopulations within *ML* CD8 T cells from patients with CHB, characterized by divergent transcriptional and functional profiles oriented toward either exhaustion (TOX^{high}) or memory T-cell differentiation (TOX^{low}). Indeed, when compared to the

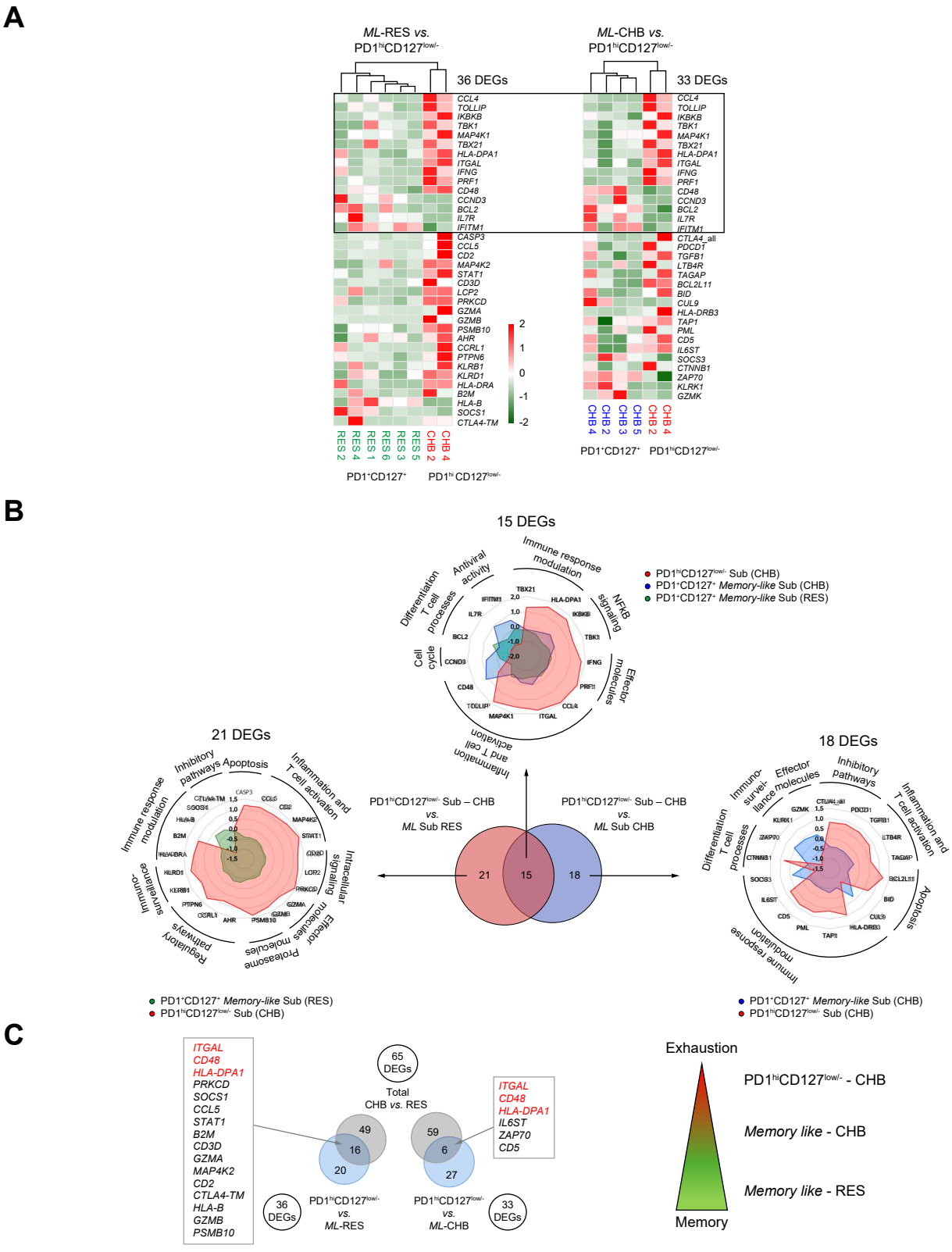

Fig. 3. Transcriptional profile of the PD1^{hi}CD127$^{low/-}$ HBV-specific CD8 T-cell subset in chronic patients. (A) Hierarchical-clustering analysis of the 36 and 33 DEGs identified comparing the PD1^{hi}CD127$^{low/-}$ (red) *vs.* *ML*-RES (green) or *ML*-CHB (blue) T-cell subsets (left and right, respectively). Up- and downregulated genes are shown in red and green, respectively. The black box shows genes shared between the two lists (n = 15). (B) Venn diagram in the center represents the 15 overlapping DEGs among the 36 and 33 above mentioned gene lists. *Top:* Radar plot of the mean z-score values of genes shared between the two lists (DEGs n = 15) grouped according to their respective functions. *Left and right:* Radar-plots of the mean z-score values of non-overlapping DEGs arising from the comparison between PD1^{hi}CD127$^{low/-}$ T cell subset (red) and *ML*-RES (green; left) or *ML*-CHB (blue; right) patients (DEGs n = 21 and n = 18, respectively). (C) Venn diagram

ML cells of resolved patients, *ML*-TOX^{high} CD8 T cells exhibited a significantly higher number of DEGs (n = 27) than that found for *ML*-TOX^{low} cells (n = 13), suggesting a transcriptional profile of *ML*-TOX^{low} cells more similar to *ML*-RES than that of *ML*-TOX^{high} cells (Fig. 4I, p = 0.006 by McNemar's test). This observation further supports the notion that *ML*-TOX^{high} and *ML*-TOX^{low} are more exhaustion- or memory-oriented, respectively.

Identification of a core gene-dysregulation signature of CD8+ T-cell exhaustion

Next, we tried to generate an aggregated T-cell exhaustion gene signature by integrating the transcriptional landscape of the different HBV-specific CD8 T-cell subsets as a continuum and considering the *ML* T cells of patients that control HBV infection (*ML*-RES) and PD1^{hi}CD127$^{low/-}$ T cells of active chronic patients as the extremes in the progressive differentiation from exhaustion to memory (Fig. 4I). We found that 11 out of the 84 genes concordantly expressed in all T-cell subsets showed a positive correlation with a progressive increase of their expression from *ML* T cells of patients able to control HBV infection, in sequence to *ML*-TOX^{low} T cells, *ML*-TOX^{high} T cells and the most dysfunctional PD1^{hi}CD127$^{low/-}$ T cells in patients with CHB (Fig. 5A and S4).

They included genes involved in inhibitory (*CD48*) and pro-inflammatory/activation processes (*CD2, CCL5, ITGAL*),[22–25] the TCR-activated tyrosine kinase *LCP2*[26] and NF-κB (*IKBKB, TBK1*)[27,28] signaling, apoptosis (*CASP3*),[29] IL4 regulatory pathway (*DUSP4*),[30] and antigen presentation (*B2M, HLA-DPA1*) (Fig. 5A and S4). Notably, 10 of these 11 genes were also included among the 36 DEGs identified by comparing the transcriptional profiles of the most extreme subsets, *i.e. ML* CD8 T cells from resolved patients and the PD1^{hi}CD127$^{low/-}$ CD8 T-cell subset from CHB patients (Fig. 5B), further supporting the notion that the 11-gene list may represent a true transcriptional exhaustion signature.

To assess whether gene deregulation is associated with an altered expression of the corresponding protein, some selected genes were tested by flow cytometry. For this purpose, dextramer-positive CD8 T cells were co-stained with monoclonal antibodies targeting the inhibitory pathway-related components CD48/CD244 and the IL4 receptor belonging to the IL4/DUSP4 signaling pathway. Increased CD244 and IL4R frequencies were detected in chronic compared to resolved infections and to FLU-specific CD8 cells from healthy controls (Fig. 6A).

Targeting the core gene-dysregulation signatures by immune modulatory interventions can improve antiviral T-cell function

To confirm whether some of the most significantly deregulated genes can actually represent suitable candidate targets for immunotherapeutic interventions, we then assessed whether HBV-specific CD8 T cells of patients with CHB were more or less sensitive *in vitro* to the modulation of the NF-kB signaling-related gene *TBK1*, and of the inhibitory pathway-related genes *CD48*/*CD244* that have already been applied with promising results in hepatocellular carcinoma[28] and head-neck squamous cell carcinoma.[22] In addition, we also tested the effect of inhibitors targeting DUSP4 and the IL4R genes belonging to the IL4 signaling pathway, whose positive effect on protective immune response has also been described in breast cancer settings[31] and in HIV infection.[32]

Notably, all tested compounds had a significant effect on HBV-specific CD8 T-cell function. Indeed, following incubation of peripheral blood mononuclear cells from CHB patients with HBV peptides covering the entire core sequence, in the presence or absence of an anti-IL4R monoclonal antibody, a TBK1 inhibitor and anti-CD244/CD48 antibodies, a significant increase in cytokine production was detected in treated compared to untreated cultures (Fig. 6B). Most of the patients displayed an increase of at least 1.5-fold, with the percentage of patients responding to treatment varying from 30% to 86%, depending on individual T-cell functions (Fig. 6C). Interestingly, 57% of patients with CHB showed an increase in the percentage of IFN-γ+ HBV-specific CD8 T cells in response to more than three simultaneous treatments (Fig. 6D, left). Functional changes induced by these immune modulatory compounds are well recapitulated by hierarchical-clustering analysis, which demonstrates a distinct distribution of patients who responded to multiple treatments. Notably, the modulatory responses induced by anti-CD244 and anti-CD48 monoclonal antibodies displayed a common clustering, reflecting the convergence of their target molecules toward a common signaling pathway, as CD48 is a ligand of CD244 and both molecules belong to the SLAM family of signaling proteins. On the other hand, despite the common involvement of TBK1 and the IL4R in the NF-κB-related signaling pathway through the engagement of the transcription factor STAT6,[33] the TBK1 inhibitor and the anti-IL4R monoclonal antibody displayed distinct distribution patterns in clustering analysis, reflecting a different magnitude of modulatory effect (Fig. 6D, right).

The combination of the TBK1 inhibitor and the anti-IL4R antibody resulted in a much greater improvement of HBV-specific CD8 T-cell responses than the individual therapeutic approaches, whereas the anti-CD48/anti-CD244 antibody combination did not reveal any synergistic or additive effect (Fig. S5A and B). Similarly to what we observed in patients with CHB, antiviral cytokine levels did not change upon incubation with the combined anti-CD48/anti-244 antibody treatment in patients who achieved functional cure with NUC therapy (Fig. S5C, left). Instead, the addition of a TBK1 inhibitor combined with an anti-IL4R monoclonal antibody to *in vitro*-expanded T cells led to a slightly greater effect, although still significantly lower than that observed in patients with CHB (Fig. S5 C, right).

representing the overlapping DEGs among different Kruskal-Wallis sub-lists: PD1^{hi}CD127$^{low/-}$ T cell subset *vs.* *ML*-RES (light blue, DEGs n = 36) and total core$_{18-27}$-specific CD8 T cells from CHB *vs*. RES patients (grey, DEGs n = 65) on the left; PD1^{hi}CD127$^{low/-}$ T cell subset *vs.* *ML*-CHB (light blue, DEGs n = 33) and total core$_{18-27}$-specific CD8 T cells from CHB *vs*. RES patients (grey, DEGs n = 65) on the right. In a scale of differentiation from exhaustion to memory, PD1^{hi}CD127$^{low/-}$ are more exhaustion-oriented, *ML*-RES more memory-oriented, and *ML*-CHB in an intermediate position. CHB, chronic hepatitis B; DEG, differentially expressed gene; ML, memory-like; PCA, principal component analysis; RES, resolved HBV infection.

Discussion

There is growing evidence that dysfunctional HBV-specific CD8 T cells are not a homogeneous population.[4–6,10] According to their antigen-specificity, HBsAg-specific CD8 T cells are rarely detectable in the peripheral blood of viremic HBeAg-negative CHB patients, likely due to maximal exhaustion and poor *in vivo* expansion. In contrast, core-specific CD8 T cells are generally more abundant and exhibit distinct phenotypes and functions compared to polymerase-specific CD8 T cells.[4–6,10] Based on phenotype, virus-specific CD8 T cells can be further subdivided into distinct CD8 T-cell subsets whose relative representation may reflect the overall protective capacity of an individual patient's CD8 T cells.[10] For example, detection of PD-1^{hi}/CD127$^{low/-}$ core-specific CD8 T cells is associated with more profound dysfunction of the overall CD8 T-cell population in HBeAg-negative CHB patients and with worse responsiveness to functional T-cell restoration strategies *in vitro*. In the same patient category, dysfunctional

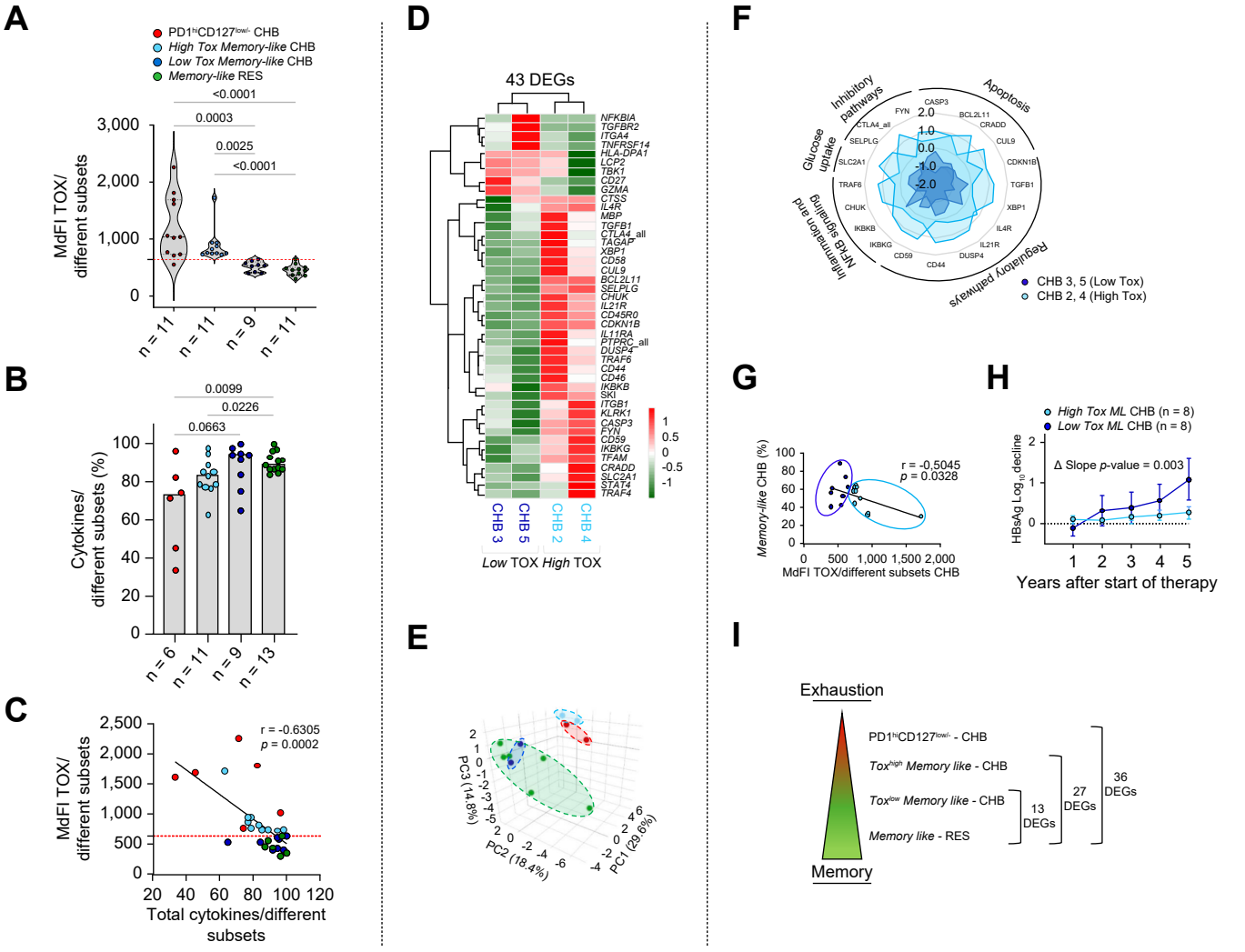

Fig. 4. TOX expression allowed us to further subdivide the *ML* PD1+CD127+ HBV-specific CD8 T-cell subset in patients with CHB. (A) TOX expression by core$_{18-27}$-specific CD8 T cells from the indicated subsets. Each dot represents an individual patient. "*High*" and "*Low*" refer to MdFI TOX values in *ML* PD1+CD127+ cells from CHB patients that are above or below 640 (red dotted line), corresponding to the maximum level observed in the RES cohort. (B) IFN-γ and TNF-α cytokine production by core$_{18-27}$-specific CD8 T cells from the above indicated subsets. (C) Inverse correlation between total cytokine production and MdFI TOX expression by the indicated subsets. Statistics by Spearman correlation test. (D) Hierarchical-clustering of the 43 DEGs identified by the comparison between *Low* TOX and *High* TOX patients (CHB3/CHB5 and CHB2/CHB4, respectively). (E) PCA representation of the 43 DEGs identified by the comparison between PD1^{hi}CD127$^{low/-}$, *ML*-TOX^{high}, *ML*-TOX^{low} and *ML*-RES subsets. (F) Radar plot depicts z-score values of selected relevant genes among the 43 DEG list grouped according to their respective functions in each *Low* TOX and *High* TOX chronic patient (blue and light blue, respectively). (G) Inverse correlation between frequencies of *ML* CD8 T-cell subsets and TOX levels from CHB patients. Statistics by Spearman correlation test. (H) Changes in serum HBsAg (log10 IU/ml) from baseline at different time points during NUC treatment in *Low* (n = 8) and *High* TOX patients (n = 8) (blue and light blue, respectively). Dots represent mean plus SEM values. Statistics by linear mixed-effects model analysis. (I) PD1^{hi}CD127$^{low/-}$ is the CD8 subset most exhaustion-oriented, followed in a progressively decreasing color scale by *ML*-TOX^{high} and *ML*-TOX^{low}, to finally end with *ML*-RES that is the most memory-oriented subset; numbers on the right show the number of DEGs for each indicated subset comparison. CHB, chronic hepatitis B; DEG, differentially expressed gene; MdFI, median fluorescence intensity; ML, memory-like; NUC, nucleos(t)ide analogue; PCA, principal component analysis; RES, resolved HBV infection.

CXCR6 positive core-specific CD8 T cells display enhanced CREM transcriptional activity, rather than TOX induction, which is typically associated with conventional exhaustion.[7] Moreover, functional attenuation of polymerase-specific CD8 T cells sustained by deregulated TGF-β signaling has been reported in chronic patients with persistently low viral loads and better control of infection.[4]

All these observations raise the issue of whether T-cell dysfunction indeed encompasses distinct cell conditions sustained by different transcription and differentiation programs that only partially overlap with those so far attributed to conventional exhaustion. They also emphasize the need to go beyond the overall transcriptional and functional profile of HBV-specific CD8 T cells to identify the specific characteristics of the different CD8 T-cell subsets that can be detected in relation to the clinical setting.

Our study addressed two main issues. First, we performed a transcriptional and functional characterization of the PD-1^{hi}/CD127$^{low/-}$ T-cell subset, which is expected to be the most severely dysfunctional, with the aim of identifying a transcriptional exhaustion/dysfunction signature and of defining the specific changes needed to drive the control of infection with HBsAg loss. Second, we analyzed the *ML* PD1+CD127+ CD8 T-cell subsets in active and resolved chronic infections to investigate whether their transcriptional and functional plasticity contributes to HBV control.

To this end, we enrolled two HBeAg-negative cohorts: patients with severe liver inflammation and active HBV replication, and patients who achieved HBsAg loss, either spontaneously or after antiviral treatment, as a reference group to identify transcriptional changes underlying disease resolution. Of note, only core-specific CD8 cells were studied because envelope- and polymerase-specific CD8 T cells are barely detectable in chronic active hepatitis B and, when detectable, their frequencies are generally too low to allow for reliable transcriptional and functional analysis of individual CD8 T-cell subsets.

We first analyzed total HBV core-specific CD8 T cells to identify a broad signature of T-cell dysfunction and then refined the analysis by focusing on the two CD8 T-cell subsets expected to be the most distant in the spectrum from more terminally exhausted, *i.e.* PD-1^{hi}/CD127$^{low/-}$, to more memory-oriented, *i.e.* the *ML*-RES CD8 T cells. Sixty-five DEGs were identified in the comparison of total CD8 T cells from CHB and resolved patients, while 20 additional DEGs were derived from the comparison of the PD-1^{hi}/CD127$^{low/-}$ *vs.* *ML*-RES subsets. Together these 85 genes define a comprehensive CD8 T-cell exhaustion/dysfunction signature that is indeed enriched in dysfunction-related transcripts already reported in other models of chronic infection.[1–4,12,14–17] Most of them belong to inflammatory and T-cell activation processes, as well as inhibitory checkpoint pathways, NF-κB signaling and effector cytotoxic functions. In line with the transcriptional data, *ML*-RES CD8 T cells showed lower TOX expression and were significantly more efficient in cytokine production than PD-1^{hi}/CD127$^{low/-}$ CD8 T cells.

Notably, the transcriptional profile observed in CHB patient CD8 T cells differs from that reported by Heim *et al.* in attenuated polymerase-specific CD8 T cells from patients with endogenous viral control, which is expected given our focus on core-specific cells from highly viremic patients, where the host environment favors terminal differentiation and severe dysfunction.

The second objective of our study was to investigate whether and to what extent the *ML* PD1+CD127+ CD8 T-cell subset is transcriptionally and functionally different in relation to the stage of infection. Our results indicate that *ML* CD8 T cells are indeed different in active *vs.* controlled chronic HBeAg-negative infections. Seventeen DEGs were identified in *ML*-CHB *vs.* *ML*-RES, enriched for dysfunction/exhaustion transcripts. Second, *ML*-CHB CD8 T cells appeared to be transcriptionally more similar to PD-1^{hi}/CD127$^{low/-}$ CD8 T cells than *ML*-RES T cells. Notably, the transcriptional differences translated into a lower capacity to produce antiviral cytokines

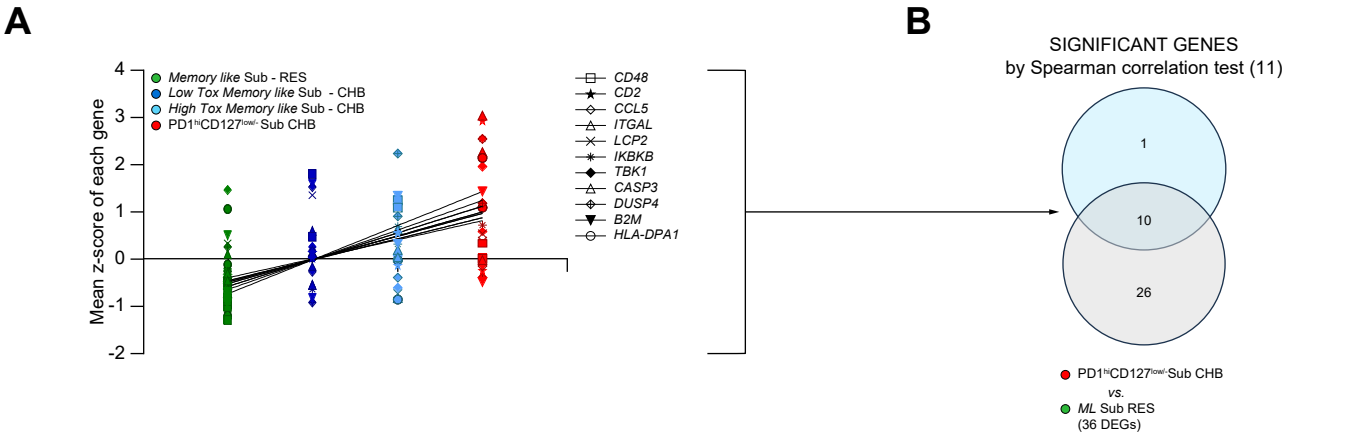

Fig. 5. Analysis of all T-cell subsets reveals a molecular signature of CD8+ T-cell exhaustion in CHB patients. (A) Analysis of 84 genes concurrently expressed across all CD8 T-cell subsets identified 11 genes displaying a significant progressive increase in expression across the indicated subset categories, with lowest levels in ML-RES patients, intermediate levels in *ML*-TOX^{low} and *ML*-TOX^{high} T cells from CHB patients, and highest levels in the PD1^{hi}CD127$^{low/-}$ subset (p <0.05 by Spearman's rank correlation test). Each symbol represents the mean z-score of individual genes. (B) Venn diagram representing the overlapping genes among the above mentioned 11 genes and the 36 DEGs obtained by the comparison of PD1^{hi}CD127$^{low/-}$ and *ML*-RES T-cell subsets. CHB, chronic hepatitis B; DEG, differentially expressed gene; ML, memory-like; PCA, principal component analysis; RES, resolved HBV infection.

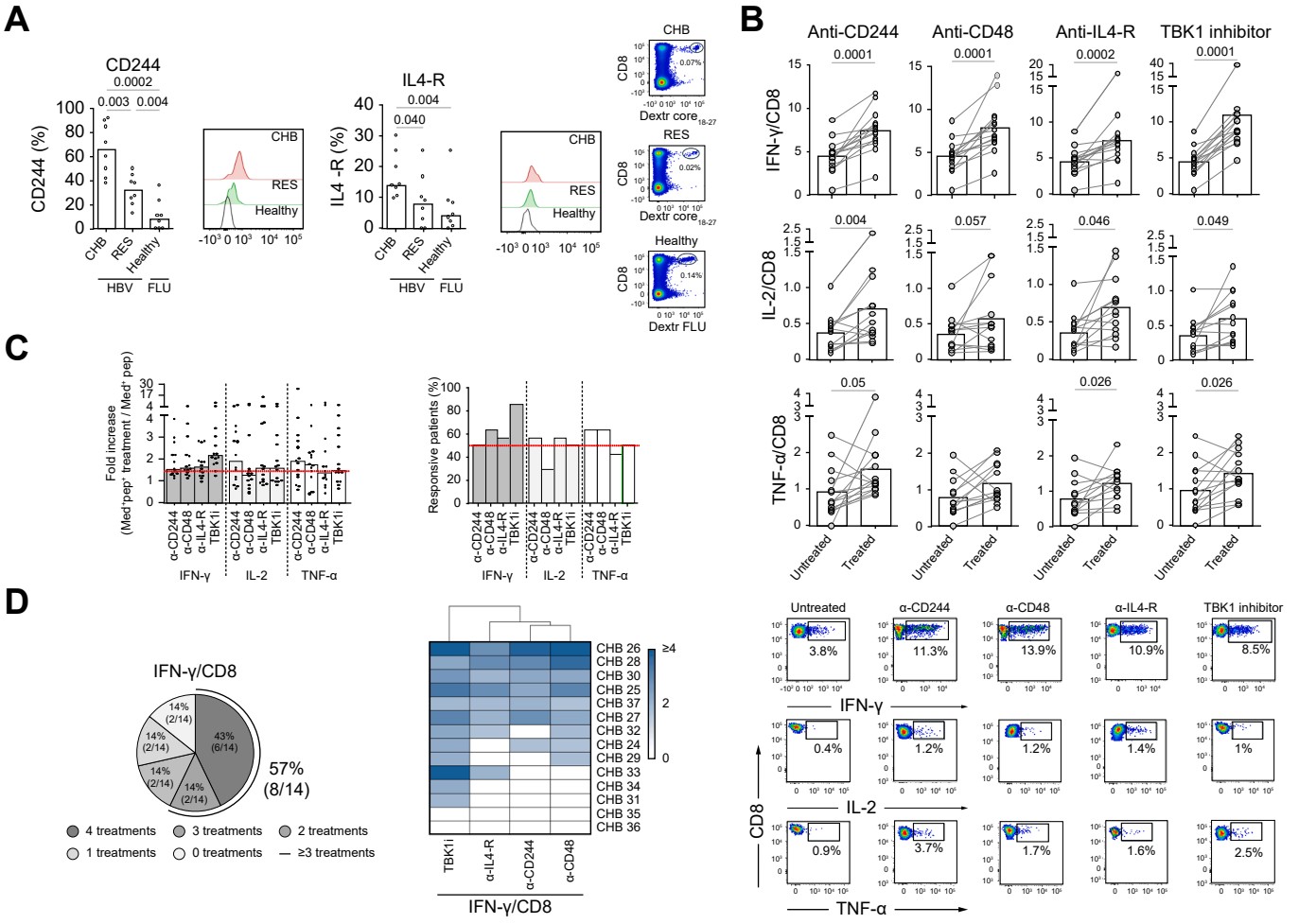

Fig. 6. Effect of immune modulatory interventions on the HBV-specific CD8 T-cell function. (A) Percentage of IL4R- and CD244-positive HBV-specific CD8 T cells from patients with CHB, RES, and FLU-specific CD8 cells from healthy controls (n = 8 for each group; Kruskal-Wallis non-parametric test). Representative examples are shown on the right. (B) Paired values (%) of cytokine-producing CD8 T cells in T-cell cultures generated by HBV core peptide stimulation in the presence or absence of an anti-IL4R monoclonal antibody, a TBK1 inhibitor and anti-CD244/CD48 antibodies (n = 14) (Wilcoxon-matched-paired test). Representative dot plots showing frequencies of IFN-γ+, TNF-α+, and IL2+ HBV-specific CD8 T cells cultured in the presence or absence of distinct modulators are illustrated on the bottom. (C) Percentage of cultures responding to a TBK1 inhibitor and to anti-IL4R, anti-CD48 and anti-244 antibodies. Patients were considered responsive to treatments when cytokine expression by CD8 T cells increased at least 1.5-fold in treated *vs.* untreated cultures. (D) Pie charts illustrate the percentage of CHB patients showing recovery of IFN-γ+ HBV-specific CD8 T-cell production induced simultaneously by multiple modulators (left). Hierarchical-clustering of IFN-γ+ HBV-specific CD8 T-cell responses in the presence of the different treatments in CHB patients (right); up and downregulated T-cell responses are shown in a color scale ranging from intense blue (maximal response) to white (negative responses), respectively. CHB, chronic hepatitis B; DEG, differentially expressed gene; FLU, influenza; RES, resolved HBV infection.

by *ML*-CHB CD8 T cells. Finally, *ML*-CHB CD8 T cells could be further divided into two distinct CD8 T-cell subsets characterized by different TOX expression levels: a first subset with higher TOX expression, transcriptionally and functionally more similar to exhausted PD-1^{hi}/CD127$^{low/-}$ CD8 T cells, and a second subset with lower TOX expression, more similar to *ML*-RES CD8 T cells.

Altogether, our data indicate that different subsets with distinctive transcriptional features can be identified within core$_{18-27}$-specific CD8 T cells, ranging from a more exhaustion-oriented PD-1^{hi}/CD127$^{low/-}$ subset followed, in a progressive scale of increasing memory differentiation, by TOX^{high} and TOX^{low} *ML* CD8 T cells from CHB patients and finally by *ML* CD8 T cells from patients achieving functional cure.

Notably, higher frequencies of TOX^{low} *ML* CD8 T cells identified CHB patients with a better serum HBsAg decline over time, suggesting an increased likelihood of resolving CHB upon NUC treatment administration in patients with TOX^{low} compared to those with TOX^{high} *ML* CD8 T cells.

The notion of progressive discrete steps of memory T-cell differentiation guided us to recapitulate the individual lists of DEGs derived from all comparisons between the different CD8 T-cell subsets into a unique, more restricted gene signature, including only those genes that displayed a progressive increase in their expression from more memory-to more exhaustion-oriented subsets. This signature comprises 11 genes (*CD48, CD2, CCL5, ITGAL, LCP2, IKBKB, TBK1, CASP3, DUSP4, B2M* and *HLA-DPA1*). Many of these genes are particularly interesting because they have been previously

reported in published transcriptome datasets of exhausted CD8 T cells in other chronic infections, including lymphocytic choriomeningitis virus (*CD48, CASP3, CCL5*)[14,15] and HCV (*DUSP4, CASP3, CCL5, HLA-DPA1, B2M, CD2*).[2,3] Remarkably, at least 5 genes from our core gene-dysregulation signature (*CD2, CCL5, ITGAL, LCP2, CD244*) were previously identified in a distinct hepatotoxic tissue-resident CD8+ T-cell subset described in the liver and characterized by a highly activated phenotype and expression of effector molecules, chemokines and exhaustion markers.[34] Ten of these 11 genes overlap with DEGs distinguishing *ML*-RES from PD-1^{hi}/CD127$^{low/-}$ subsets. Therefore, targeting these deregulated genes may represent an ideal CD8 functional reconstitution strategy. In line with this prediction, administration of a TBK1 inhibitor or anti-IL4R or anti-CD244/CD48 antibodies to *in vitro*-expanded T cells led to improved cytokine production in most of the tested CHB patients, with the TBK1 inhibitor showing slightly superior effects, further potentiated when combined with anti-IL-4R.

Interestingly, restoration of T-cell function has previously been reported in hepatocellular carcinoma,[28] gastric cancer[24] and head-neck squamous cell carcinoma[22] through the modulatory effect of TBK1, CCL5/CCR5 and CD48/CD244 inhibitors. Moreover, targeting DUSP4 and the IL4R genes belonging to the IL4 signaling pathway sensitized cancer cells to anti-cancer therapy and strengthened protective immune responses in breast cancer,[31] and in HIV infection.[32] These observations suggest that these compounds may be promising for restoring exhausted CD8 T cells in chronic HBV infection, warranting further studies in larger patient cohorts to validate their potential as immunotherapeutic targets.

Affiliations

[1]*Department of Medicine and Surgery, University of Parma, Parma, Italy;* [2]*Laboratory of Viral Immunopathology, Unit of Infectious Diseases and Hepatology, Azienda Ospedaliero-Universitaria of Parma, Parma, Italy;* [3]*Lyon Hepatology Institute, Lyon, France;* [4]*UMR U1350 PaThLiv, Lyon, France;* [5]*Division of Gastroenterology and Hepatology, Foundation IRCCS Ca' Granda Ospedale Maggiore Policlinico, Milan, Italy;* [6]*Department of Medicine and Surgery, Unit of Neuroscience, Interdepartmental Center of Robust Statistics (Ro.S.A.), University of Parma, Parma, Italy;* [7]*CRC "A. M. and A. Migliavacca" Center for Liver Disease, Department of Pathophysiology and Transplantation, University of Milan, Milan, Italy;* [8]*Department of Hepatology, Hôpital Croix-Rousse, Hospices Civils de Lyon, Lyon, France;* [9]*University of Lyon Claude Bernard 1 (UCLB1), Lyon, France;* [10]*Dip. SCIAC, University of Rome La Sapienza, Rome, Italy*

Abbreviations

CHB, chronic hepatitis B; DEGs, differentially expressed genes; ML, memory-like; NUC, nucleos(t)ide analogues; RES, resolved HBV infection.

Financial support

This work was supported by the PRIN projects from the Italian Ministry of the University and Research (protocol code n. 2017MPCWPY and 2022FMESXL), and by a grant from the European Union's Horizon 2020 research and innovation programme (grant agreement no. 848223).

Conflicts of interest

PL: advisor and speaker bureau for Roche pharma/diagnostics, Gilead Sciences, GSK, Abbvie, Janssen, Myr Pharma, EIGER, Antios, Aligos, Vir, Grifols, Altona, Roboscreen; CF: Grant: Gilead, Abbvie. Consultant: Gilead, Abbvie, Vir Biotechnology Inc, Arrowhead, Transgene, BMS; ML: Grant: Ipsen. Advisor and speaker bureau for Gilead, Roche, Abbvie, Ipsen, Evotec/Sanofi. The remaining authors disclose no conflicts.

Please refer to the accompanying ICMJE disclosure forms for further details.

Authors' contributions

MR, AV, CT: execution of experiments, acquisition of data, statistical analysis, analysis and interpretation of data. FG, MLP: execution of transcriptomic experiments, analysis of data. ED, DS, AA: recruitment and characterization of the patients. EAG, AP, VR, AM, AP, SD, BF: analysis of data. DL: administrative support. GP: statistical analysis. PF, GM, PL: interpretation of data, critical revision of the manuscript. ML: study concept and design, critical revision and editing of the manuscript. CF: study concept and design, critical revision and editing of the manuscript, obtained funding, study supervision and interpretation of data. CB: study concept and design, analysis and interpretation of data, writing of the manuscript.

Acknowledgements

We Thank the Plateforme Anatomopathologie Recherche Lyon-Est at the Cancer Research Center of Lyon (CRCL) INSERM U1052 for assistance in the Nanostring N-Counter Experiments.

Supplementary data

Supplementary data to this article can be found online at https://doi.org/10.1016/j.jhepr.2025.101705.

References

Author names in bold designate shared co-first authorship

[1] **McLane LM**, **Abdel-Hakeem MS**, Wherry EJ. CD8 T cell exhaustion during chronic viral infection and cancer. Annu Rev Immunol 2019;37:457–495.

[2] **Hensel N**, **Gu Z**, **Sagar**, et al. Memory-like HCV-specific CD8+ T cells retain a molecular scar after cure of chronic HCV infection. Nat Immunol 2021;22:229–239.

[3] Tonnerre P, Wolski D, Subudhi S, et al. Differentiation of exhausted CD8+ T cells after termination of chronic antigen stimulation stops short of achieving functional T cell memory. Nat Immunol 2021;22:1030–1041.

[4] **Heim K**, **Sagar**, Sogukpinar Ö, et al. Attenuated effector T cells are linked to control of chronic HBV infection. Nat Immunol 2024;25:1650–1662.

[5] **Schuch A**, **Alizei ES**, **Heim K**, et al. Phenotypic and functional differences of HBV core-specific versus HBV polymerase-specific CD8+ T cells in chronically HBV-infected patients with low viral load. Gut 2019;68:905–915.

[6] Hoogeveen RC, Robidoux MP, Schwarz T, et al. Phenotype and function of HBV-specific T cells is determined by the targeted epitope in addition to the stage of infection. Gut 2019;68:893–904.

[7] **Bosch M**, **Kallin N**, Donakonda S, et al. A liver immune rheostat regulates CD8 T cell immunity in chronic HBV infection. Nature 2024;631:867–875.

[8] Khakpoor A, Ni Y, Chen A, et al. Spatiotemporal differences in presentation of CD8 T cell epitopes during hepatitis B virus infection. J Virol 2019;93.

[9] **Bert N Le**, **Gill US**, **Hong M**, et al. Effects of hepatitis B surface antigen on virus-specific and global T cells in patients with chronic hepatitis B virus infection. Gastroenterology 2020;159:652–664.

[10] **Rossi M**, **Vecchi A**, **Tiezzi C**, et al. Phenotypic CD8 T cell profiling in chronic hepatitis B to predict HBV-specific CD8 T cell susceptibility to functional restoration in vitro. Gut 2023;72:2123–2137.

[11] Lampertico P, Agarwal K, Berg T, et al. EASL 2017 Clinical Practice Guidelines on the management of hepatitis B virus infection. J Hepatol 2017;67:370–398.

[12] Fisicaro P, Barili V, Montanini B, et al. Targeting mitochondrial dysfunction can restore antiviral activity of exhausted HBV-specific CD8 T cells in chronic hepatitis B. Nat Med 2017;23:327–336.

[13] Olivier J, May WL, Bell ML. Relative effect sizes for measures of risk. Commun Stat Theor Methods 2017;46:6774–6781.

[14] Doering TA, Crawford A, Angelosanto JM, et al. Network analysis reveals centrally connected genes and pathways involved in CD8+ T cell exhaustion versus memory. Immunity 2012;37:1130–1144.

[15] Wherry EJ, Ha S-J, Kaech SM, et al. Molecular signature of CD8+ T cell exhaustion during chronic viral infection. Immunity 2007;27:670–684.

[16] **Andreata F**, **Laura C**, **Ravà M**, et al. Therapeutic potential of co-signaling receptor modulation in hepatitis B. Cell 2024;187:4078–4094.e21.
[17] **Narmada BC**, **Khakpoor A**, **Shirgaonkar N**, et al. Single-cell landscape of functionally cured chronic hepatitis B patients reveals activation of innate and altered CD4-CTL-driven adaptive immunity. J Hepatol 2024;81:42–61.
[18] Ilangumaran S, Bobbala D, Ramanathan S. SOCS1: regulator of T cells in autoimmunity and cancer. 2017. p. 159–189.
[19] Wada T. Downregulation of CD5 and dysregulated $CD8^+$ T-cell activation. Pediatr Int 2018;60:776–780.
[20] **Hop HT**, **Huy TXN**, Reyes AWB, et al. Interleukin 6 promotes *Brucella abortus* clearance by controlling bactericidal activity of macrophages and $CD8^+$ T cell differentiation. Infect Immun 2019;87.
[21] Groom JR, Luster AD. CXCR3 in T cell function. Exp Cell Res 2011;317:620–631.
[22] Agresta L, Lehn M, Lampe K, et al. CD244 represents a new therapeutic target in head and neck squamous cell carcinoma. J Immunother Cancer 2020;8:e000245.
[23] Binder C, Cvetkovski F, Sellberg F, et al. CD2 immunobiology. Front Immunol 2020;11.
[24] Aldinucci D, Casagrande N. Inhibition of the CCL5/CCR5 Axis against the progression of gastric cancer. Int J Mol Sci 2018;19:1477.
[25] **Zhang J**, **Wang H**, Yuan C, et al. ITGAL as a prognostic biomarker correlated with immune infiltrates in gastric cancer. Front Cell Dev Biol 2022;10.
[26] Wang Z, Peng M. A novel prognostic biomarker LCP2 correlates with metastatic melanoma-infiltrating CD8+ T cells. Sci Rep 2021;11:9164.
[27] **Yang L**, **Zhou L**, Li F, et al. Diagnostic and prognostic value of autophagy-related key genes in sepsis and potential correlation with immune cell signatures. Front Cell Dev Biol 2023;11.
[28] **Jiang Y**, **Chen S**, **Li Q**, et al. TANK-binding kinase 1 (TBK1) serves as a potential target for hepatocellular carcinoma by enhancing tumor immune infiltration. Front Immunol 2021;12.
[29] Christgen S, Tweedell RE, Kanneganti T-D. Programming inflammatory cell death for therapy. Pharmacol Ther 2022;232:108010.
[30] Zhao Y, Cai H, Ding X, et al. An integrative analysis of the single-cell transcriptome identifies DUSP4 as an exhaustion-associated gene in tumor-infiltrating CD8+ T cells. Funct Integr Genomics 2023;23:136.
[31] **Gaggianesi M**, **Turdo A**, Chinnici A, et al. IL4 primes the dynamics of breast cancer progression via DUSP4 inhibition. Cancer Res 2017;77:3268–3279.
[32] **Jackson RJ**, **Worley M**, Trivedi S, et al. Novel HIV IL-4R antagonist vaccine strategy can induce both high avidity CD8 T and B cell immunity with greater protective efficacy. Vaccine 2014;32:5703–5714.
[33] **Chen H**, **Sun H**, **You F**, et al. Activation of STAT6 by STING is critical for antiviral innate immunity. Cell 2011;147:436–446.
[34] Nkongolo S, Mahamed D, Kuipery A, et al. Longitudinal liver sampling in patients with chronic hepatitis B starting antiviral therapy reveals hepatotoxic CD8+ T cells. J Clin Invest 2023;133(1):e158903.

Keywords: Chronic HBV infection; CD8 T-cell exhaustion; T-cell functional reconstitution; T-cell heterogeneity.
Received 8 July 2025; received in revised form 21 November 2025; accepted 26 November 2025; Available online 4 December 2025